Long Noncoding RNA FER1L4 Promotes Papillary Thyroid Cancer Progression by Targeting miR-612/CDH4 Axis

Luyao Wu
Jiangsu Province Hospital and Nanjing Medical University First Affiliated Hospital
Yu Ding
Jiangsu Province Hospital and Nanjing Medical University First Affiliated Hospital
Xi Zhuang
Jiangsu Province Hospital and Nanjing Medical University First Affiliated Hospital
Jingsheng Cai
Jiangsu Province Hospital and Nanjing Medical University First Affiliated Hospital
Houchao Tong
Jiangsu Province Hospital and Nanjing Medical University First Affiliated Hospital
Yan Si
Jiangsu Province Hospital and Nanjing Medical University First Affiliated Hospital
Hao Zhang
Jiangsu Province Hospital and Nanjing Medical University First Affiliated Hospital
Xiaoting Wang
Jiangsu Province Hospital and Nanjing Medical University First Affiliated Hospital
Meiping Shen (shenmeiping@jsph.org.cn)
Jiangsu Province Hospital and Nanjing Medical University First Affiliated Hospital

Research

Keywords: Papillary thyroid cancer, long noncoding RNA, FER1L4, miR-612, CDH4

Posted Date: February 9th, 2021

DOI: https://doi.org/10.21203/rs.3.rs-177558/v1

Abstract

Background: Long noncoding RNAs (lncRNAs) have emerged as crucial regulators in various cancers. However, the functional roles of most lncRNA in papillary thyroid cancer (PTC) are not detailly understood. This study aims to investigate the biological functions and the molecular mechanism of lncRNA FER1L4 in PTC.

Methods: The expression of FER1L4 in PTC was determined via operating RT-PCR assays. Meanwhile, the clinical significance of FER1L4 in PTC patients was described. The biological functions of FER1L4 on PTC cells were evaluated by gain and loss of function experiments. Moreover, animal experiments were performed to reveal the effect on tumor growth. Subcellular distribution of FER1L4 was determined by fluorescence in situ hybridization and subcellular localization assays. Luciferase reporter assay and RNA immunoprecipitation assay were applied to define the relationship between FER1L4, miR-612, and CDH4.

Results: Upregulated expression of FER1L4 in PTC tissues was correlated with higher lymph node metastasis rate (p=0.020), extrathyroidal extension (p=0.013), and advanced TNM stage (p=0.013). In addition, knockdown of FER1L4 suppressed PTC cell proliferation, migration and invasion, whereas ectopic expression of FER1L4 inversely promoted these processes. Mechanistically, FER1L4 could competitively bind with miR-612 to prevent the degradation of its target gene Cadherin 4 (CDH4). This condition was further confirmed in the rescue assays.

Conclusions: This study firstly demonstrates FER1L4 plays an oncogenic role in PTC via FER1L4-miR-612-CDH4 axis and may provide a new therapeutic and diagnostic target for PTC.

Background

Thyroid cancer (TC) is the most frequent malignancy of the endocrine system, ranking ninth in the incidence of tumors worldwide (1). Papillary thyroid carcinoma (PTC) is the major pathological type, accounting for more than 85% of differentiated thyroid cancer (DTC) (2). With the improvement of diagnostic technology such as ultrasound, the detection rate of DTC has been significantly increased during the last few decades (3). However, DTC patients usually have an excellent prognosis, with 10-year disease-specific survival rates over 90% (4). Of note, about 10% of patients with DTC have distant metastases to lungs or bones at diagnosis or during follow-up, resulted in poor prognosis (5). Meanwhile, the incidence of larger tumors also elevates, which is not likely to be explained by the screening effect (3). And to date, the etiology of thyroid cancer remains unclear. Thus, exploring the molecular basis of PTC pathogenesis and progression is crucial for developing more effective therapeutic and diagnostic targets to PTC.

Long noncoding RNAs (lncRNAs) refer to the noncoding portions of the genome without protein-coding signatures, which transcript longer than 200 nucleotides (6). LncRNAs are considered to regulate varieties of physiological and pathological functions, including the occurrence and progression of cancers (7, 8). In recent years, aberrant expression of lncRNA has been found in various tumors. For example, in

hepatocellular carcinoma, lncRNA AY could promote hepatocellular carcinoma metastasis via induction of chromatin modification for ITGAV transcription (9). In addition, it was reported upregulated expression of lncRNA BCRT1 in breast cancer remarkably accelerates tumor growth and metastasis by acting as a sponge for miR-1303 to attenuate its repressive effect on PTBP3 and by mediating hypoxia-induced malignant properties of breast cancer cells (10). However, researches on the underlying role of lncRNA in PTC carcinogenesis are still lacking yet.

LncRNA performs its complex biological functions through multiple ways, which is closely related with its subcellular localization (11). For lncRNAs largely localized in the cytoplasm, they mainly function by acting as decoys for miRNAs, in which lncRNA could control miRNA availability for its target gene, so named as competing endogenous RNAs (ceRNA) either (12). In case of thyroid cancer, lncRNA-GAS8-AS1, located in the cytoplasm of PTC cells, was found that could promote autophagy of PTC cells by sponging oncogenic miR-187-3p and miR-1343-3p and upregulating the expression of ATG5 and ATG7 respectively (13). In this study, lncRNA fer-1 like family member 4 (FER1L4) is identified as an oncogene which promotes PTC cell proliferation, migration and invasion via functioning as ceRNA for tumor suppressor, miR-612.

Cadherin 4, also named as retinal cadherin, is a classical cadherin from the cadherin superfamily consisting of epithelial-cadherin (E-cadherin, CDH1), neural-cadherin (N-cadherin, CDH2), placental-cadherin (P-cadherin, CDH3), and so on (14). Cadherins are transmembrane glycoproteins responsible for cell-cell adhesion, tissue pattering and carcinogenesis (15). Previous researches indicate that cadherins could bind to catenin proteins and then form the cadherin-catenin complex to activate the catenin signaling or not, and involve in the epithelial-mesenchymal transition (EMT) process (16). However, the function of CDH4 in PTC remains unknown and its role in above process, however, is still controversial (17). In the present study, CDH4 is considered as the downstream target of miR-612, which mediates the promoting role of FER1L4 in PTC cells.

Materials And Methods

Patients and tissue samples

Eighty thyroid papillary cancer tissues and adjacent normal tissues were collected from 80 patients with PTC who received operation on the First Affiliated Hospital of Nanjing Medical University (NMU). None of the patients underwent any other treatment but surgery. All collected tissue samples were immediately snap frozen in liquid nitrogen and stored at −80 °C until required. Our study was approved by the Ethics Committee of the First Affiliated Hospital of NMU.

Cell lines

Four PTC cell lines (K-1, TPC-1, B-CPAP and IHH-4) and a normal thyroid follicular epithelium cell line (Nthy-ori3-1) were purchased from the American Type Culture Collection (ATCC). K-1, B-CPAP and Nthy-

ori3-1 cells were cultured in RPMI1640 medium (Gibco, USA), while TPC-1 cells were cultured in DMEM with high glucose (Gibco, USA). Mixture (1:1) of RPMI 1640 and DMEM was used to culture the IHH-4 cell line. 1% antibiotics (100 U/ml penicillin and 100 mg/ml streptomycin) and 10% fetal bovine serum (Gibco, USA) were added to all of the above culture media. All cell lines were incubated in a humidified atmosphere at 37 °C containing 5% CO2.

RNA extraction and quantitative real-time PCR analysis

Total RNA was extracted from tissues and cultured cell lines using TRIzol reagent (Invitrogen, USA). A PrimeScript RT reagent kit (Takara, Japan) was used to synthesize cDNA. MiRNAs were reverse transcribed after polyadenylation using Revert Aid First Strand cDNA Synthesis Kit (Thermo Scientific, MA, USA). Quantitative real-time PCR (qRT-PCR) was performed with AceQ qPCR SYBR Green Master Mix (Vazyme, China). Results were calculated using the $2^{-\Delta\Delta CT}$ method and normalized to the expression of GAPDH for mRNA or U6 for miRNA. Primers used in the study were listed in Additional file 1 Table S1.

Cell transfection

PTC cells were transfected with 50nm siRNAs and plasmid vectors when they grew to 30-40% density using Lipofectamine 3000 (Invitrogen, Carlsbad, CA, USA) according to the manufacturer's recommendations. In this study, siRNAs, miR-612 mimics, miR612 inhibitor and correspondent negative control were purchased from Genepharma. After 48h transfection, the cells were harvested for performing the following experiments. Plasmid vectors encoding FER1L4 and biologically active short hairpin RNAs (shRNA) targeting FER1L4 or CDH4 were generated either (Genepharma, Shanghai, China). Stable cell lines were obtained by using 2μg/ml puromycin (Sigma-Aldrich, St-Louis, Missouri, USA) for about three weeks. Nucleotide sequences mentioned above were listed in Additional file 2 Table S2.

Cell proliferation assay

In order to investigate the effect on cell proliferation of corresponding treatment to K-1 and TPC-1 cells, cell counting kit 8 (CCK8) assay, colony formation assay and 5-Ethynyl-2'-deoxyuridine (EdU) incorporation assay were applied. Detailed information has been described before (18).

Animal experiment

Four-week female BALB/c nude mice were purchased from the Animal Center of NMU and all experiments were approved by Committee on the Ethics of Animal Experiments of the Nanjing Medical University. For the tumorigenicity studies, a total of 20 mice were randomly assigned, stable transfected cells (1×10^6 cells/100μl of PBS) were subcutaneously injected into the flank of the nude mice. The tumor volume was measured every 4 days and calculated by the formula: volume = (length × width2)/2.

Immunohistochemical (IHC) analysis

All specimens were fixed in 4% formalin and then embedded in paraffin. After blocking endogenic peroxides and proteins, these sections were incubated with primary antibodies specific for Ki-67 (Abcam) or CDH4 (Abclonal) at 4°C overnight, lastly were counterstained with hematoxylin after incubating with the secondary antibodies at 37 °C for 1 h. Random images were obtained using a light microscope. (Olympus Corp. Tokyo, Japan)

Cell migration and invasion assays

Transwell chambers (Corning, USA) coated with or without Matrigel (BD Bioscience, USA) were used to evaluate the function of genes on cell migrative and invasive ability. Meanwhile, cell motility also examined by wound healing assay. Detailed information has been described before (18).

Flow cytometric analysis

Treated cells were collected for Flow cytometric analysis. According to the protocol of the reagent (MultiSciences, China), APC-Annexin V and Propidium Iodide (PI) were used to stain cells, and the rate of apoptosis was analyzed by a flow cytometry (FACScan, BD Biosciences). For cell cycle analysis, treated cells was stained by PI-staining solution, and then the percentages of cells in G_0–G_1, S, and G_2–M phase were counted.

Western blot assay and antibodies

Western blot assay was performed following previous protocol. The primary antibody used were listed in Additional file 3 Table S3.

Subcellular fractionation and Fluorescence in situ hybridization (FISH)

The separation and purification of cytoplasmic and nuclear was implemented using the PARIS Kit (Life Technologies, USA) according to the manufacturer's instructions. For the FISH assay, The Cy3-labeled FER1L4 probe used in our study was synthesized by (RiBo Ltd, Guangzhou, China). Briefly, the prepared cells were incubated with specific probes at 37 °C overnight after fixation and permeabilization. Finally, the nuclei were stained by DAPI and observed using confocal microscope.

Dual-luciferase reporter assay

The sequences of FER1L4 and CDH4 3'-UTR containing wild-type or mutated miR-612 binding sites were synthesized and loaded into a pGL3 luciferase reporter vector (Promega, USA). TPC-1 cells (1×10^5) were cotransfected with miRNA mimics or control, and the luciferase reporter vectors. After 48h of incubation, the luciferase activities were measured using a Dual-Luciferase Reporter Assay System (Promega, Wisconsin, USA). Relative luciferase activity was normalized to *Renilla* luciferase.

RNA immunoprecipitation (RIP) assay

For detecting whether FER1L4 participates in the RNA-induced silencing complex mediated by miRNA, RIP assays were conducted using the Magna RIPTM RNA-binding protein immunoprecipitation kit (Millipore, USA). Briefly, the prepared cells were lysed and incubated with anti-Ago2 (Abcam, CA, MA, USA) or IgG antibody at 4 °C overnight. Then, cell lysates were incubated with the protein A magnetic beads for 4h. The coprecipitated RNAs were collected for qRT-PCR analysis.

Bioinformatic analyses

The gene expression data of PTC from TCGA (http://cancergenome.nih.gov/) was used to explore abnormally expressed lncRNA. The target miRNAs of FER1L4 were predicted using starbase (http://starbase.sysu.edu.cn/), miRcode (http://www.mircode.org/) and RegRNA2.0 (http://regrna2.mbc.nctu.edu.tw/). Meanwhile, miRWALK (http://zmf.umm.uni-heidelberg.de/apps/zmf/mirwalk/) was applied to determine the downstream targets of miR-612.

Statistics analysis

The data are described by the mean ± standard deviation (SD) in three independently experiments. For comparing statistical differences, Student's t-tests, Pearson Chi-square test, Wilcoxon test were performed as appropriate using SPSS v22.0 and GraphPad Prism 6. Spearman's correlation analysis was selected to analyze the correlations among FER1L4, miR-612 and CDH4. P value less than 0.05 is considered statistically significant.

Results

FER1L4 is upregulated in PTC and associates with advanced stage

To identify genes that have pivotal roles in PTC tumorigenesis, expression signature of genes was screened based on TCGA database. In this study, we observed preferential upregulation of lncRNA FER1L4 in TC tissues (n=513) compared with normal tissues (n=58; Fig. 1A-B). Moreover, FER1L4 also showed concordance in a pattern of expression in PTC cell lines compared with an immortalized thyroid

follicular epithelium cell line Nthy-ori-1 (Fig. 1C). Importantly, identical results were also detected via measuring the expression in 80 paired PTC tissues and adjacent normal tissues, in which 79 percent of patients exhibited higher expression of FER1L4 in PTC tissues (Fig. 1D). Furthermore, through investigating the clinical significance of FER1L4 in 80 PTC patients, it showed enhanced expression of FER1L4 correlated with higher lymph node metastasis rate (p=0.020), extrathyroidal extension (p=0.013), and advanced TNM stage (p=0.013) (Additional file 4: Table S4). In addition, analysis of TCGA cohort suggested that upregulation of FER1L4 predicted poor histological type, deeper tumor invasion depth (T stage), higher lymph node metastasis rate (N stage) and advanced TNM stage either (Fig. 1E-H). Therefore, these results supported an oncogenic role for FER1L4 in PTC.

FER1L4 promotes PTC cell growth and motility both in vivo and in vitro

To elucidate the potential function of FER1L4, TPC-1 and K-1 cells were transfected with FER1L4 targeting small interfering RNA (siRNA) or control siRNA (Fig. 2A). Firstly, CCK8 assays demonstrated that knockdown of FER1L4 suppressed the cell growth of TPC-1 and K-1 cells (Fig. 2B). Meanwhile, overexpression of FER1L4 showed enhanced proliferative capacity of cells transfected with plasmid vectors encoding FER1L4 (Fig. 2C-D). Additionally, colony-formation assays indicated that silencing FER1L4 significantly reduced the colony numbers (Fig. 2E), while upregulation of FER1L4 drastically enhanced them (Fig. 2F). Moreover, EdU incorporation assays showed an analogous mode as above, in which EdU positive cell numbers were progressively reduced following depletion of FER1L4 (Fig. 2G), whereas overexpression of FER1L4 resulted in an increase of these cells (Fig. 2H). Importantly, there is successfully identifies that decreased apoptosis and cell-cycle promotion are two factors that could contribute to the outgrowth of cancer cell. Herein, we performed flow cytometric assays to examine the role of FER1L4 in these properties. Notably, knockdown of FER1L4 showed a growing number of apoptotic cells in TPC-1 and K-1 cells treated with FER1L4 targeting siRNA (Fig. 3A; Additional file 5: Fig S1A). Apart from increased cell apoptosis, FER1L4-knockdown PTC cells had a significantly higher percentage of cells in the S phase with detriment to the G0/1 phase cells than did cells expressed a negative control RNA, which indicated the induction of cell arrest at S phase after silencing FER1L4 (Fig. 3B). Remarkably, Western blot analysis showed depletion of FER1L4 was accompanied with reduced expression of apoptotic marker like Bcl2, along with enhanced expression of pro-apoptosis protein like Bax. Meanwhile, the expression level of S-phase checkpoint proteins such as CyclinA2 and CDK2 were also decreased in FER1L4 silenced PTC cells (Fig. 3C; Additional file 5: Fig S1B). In parallel, in order to investigate the function of FER1L4 in vivo, TPC-1 cells transduced with lentivirus vectors carrying FER1L4 shRNA or scrambled sequence were subcutaneously injected into the flank of 4 weeks female nude mice. It showed that depletion of FER1L4 decreased the tumor growth of TPC-1 cells (Fig. 3D), and the tumor size and final tumor weight in implanted tumors were significantly decreased in knockdown group (Fig. 3E-F). Furthermore, immunohistochemistry analysis of orthotopically implanted tumors showed

diminished numbers of Ki67-positive cells by inhibition of FER1L4 (Fig. 3G). Thus, these data indicated that FER1L4 has a critically promoting role in PTC cell growth.

The molecular mechanisms behind the capacity for tumor cells to metastasize efficiently is an important topic. Therefore, it is necessary to evaluate whether FER1L4 involves in PTC metastasis. First, wound healing assays showed that FER1L4-knockdown led to attenuated migration of PTC cells (Fig. 3H; Additional file 5: Fig S1C). Transwell assays further suggested that loss of FER1L4 resulted in reduced numbers of cells getting through the chamber (Fig. 3I), whereas ectopic expression of FER1L4 showed elevated cell numbers (Fig. 3J). Consequently, our results suggested that FR1L4 essentially involves in the early metastasis of PTC cells.

miR-612 is sponged by FER1L4 in PTC

Long non-coding RNA plays many roles in cellular physiology which is partially dependent on its subcellular location. In this study, we found FER1L4 mainly located in the cytoplasm of PTC cell by conducting in situ hybridization assay and subcellular fractionation assay, which suggested that FER1L4 may regulate the expression of targets at the post-transcriptional level (Fig. 4A-B; Additional file 5: Fig S1D). Then, combining gene expression profiling from TCGA database, along with prediction tools such as regRNA2.0 (19), miRcode (20) and starbase (21), we selected five potential miRNAs (miR-612, miR-140-3p, miR-92a-3p, miR-196b-5p and miR-784-3p) with binding sites in FER1L4 sequences (Fig. 4C; Additional file 6: Fig S2A). However, only miR-612, miR-140-3p and miR-784-3p could bind with FER1L4 transcripts, which we tested through conducting dual luciferase reporter assays (Fig. 4D). Meanwhile, knockdown of FER1L4 also showed upregulated expression of miR-612, miR-140-3p and miR-784-3p in TPC-1 cells (Fig. 4E). Nevertheless, considering the highest binding affinity between FER1L4 and miR-612, we exclusively chosen miR-612 for further study. As illustrated in Figure 4F, the binding sequence of miR-612 to FER1L4 were mutated and then fused into the luciferase reported vector (MUT type). Notably, mutation of the miR-612 binding sites in FER1L4 3'UTR abolished the suppressive effects to FER1L4-driven luciferase activity by miR-612 mimics in PTC cells (Fig. 4F). In addition, overexpression of FER1L4 caused reduction of miR-612 expression either (Fig. 4G). RNA-binding protein immunoprecipitation (RIP) assay further revealed that FER1L4 was successfully immunoprecipitated from cell extracts using Ago2 antibody (Fig. 4H). On the other hand, a significant inverse correlation between FER1L4 and miR-612 was acquired through analyzing of 20 PTC tissue samples (R^2=0.38, P=0.0036) (Additional file 6: Fig S2B). Taken together, these studies identified that FRE1L4 could sequester miR-612 away to its targets, therefore involves in PTC tumorigenesis.

miR-612 is sufficient and necessary for FER1L4-induced effects

Although above data confirmed miR-612 was one of the targets of FER1L4, but the function of miR-612 in PTC has never been determined yet. First, the expression of miR-612 was downregulated in K-1 and TPC-1 cells compared with normal cell line Nthy-ori-1 (Fig. 4I). Next, in order to investigate whether miR-612 modulates the biological behavior of PTC cells, the expression of miR-612 was successfully attenuated by miR-612 inhibitor and artificially enhanced by miR-612 mimics (Fig. 4J). Overexpression of miR-612 inhibited cell growth (Fig. 5A-B) and colony formation (Fig. 5C; Additional file 6: Fig S2C), whereas inhibition of miR-612 showed opposite effect. Flow cytometric assays also indicated reintroduction of miR-612 into PTC cells induced cell apoptosis (Fig. 5D) and cell cycle arrest in S phase (Fig. 5E). Moreover, transwell assays also indicated ectopic expression of miR-612 progressively inhibited PTC cell migration and invasion (Fig. 5F; Additional file 6: Fig S2D). We next sought to explore whether FER1L4 promotes PTC cell growth and motility via regulating miR-612. PTC cells were co-transfected with siRNA against FER1L4 and miR-612 inhibitor, and the resulting cells were subjected to CCK8 assay and transwell assay. It revealed the inhibitory effect on PTC cell by knockdown of FER1L4 was nullified by miRNA-612 inhibitor (Fig. 5G-J; Additional file 6: Fig S2E-F). As a result, these data unveiled the mechanism of promotive effects on PTC cells mediated by FER1L4 is to sponge miR-612.

FER1L4 upregulates CDH4 expression via inhibition of miR-612

The downstream target of miR-612 was predicted by miRwalk (22), and CDH4 was identified with potential miR-612 binding sites. Intriguingly, the RNA level of CDH4 was not influenced by silencing FER1L4 or overexpression of miR-612 (Fig. 6A-B). However, the protein level of CDH4 was significantly diminished after decreasing FER1L4 expression or enhancing the expression of miR-612 (Fig. 6C; Additional file 7: Fig S3A-B). To this end, it may suggest miR-612 could negatively regulate CDH4 expression through translational repression. For subsequent investigation, dual luciferase reporter assays were performed to validate whether miR-612 directly binds to CDH4 in PTC cells. As presented in Figure. 6D, miR-612 seed sequence in CDH4 3'UTR were mutated (MUT-CDH4), and then the mutated 3'UTR sequence and the wild type 3'UTR sequence of CDH4 (WT-CDH4) were fused into a plasmid vector respectively. The luciferase activity was significantly decreased following co-transfection of miR-612 mimics and WT-CDH4 reporter vector, which is blocked by MUT-CDH4 (Fig. 6D). Of note, diminished expression of CDH4 protein in FER1L4 silenced PTC cells was rescued by co-transfection with miR-612 inhibitor (Fig. 6E; Additional file 7: Fig S3C). Moreover, a negative correlation between FER1L4 and CDH4 (R^2=0.56, $P < 0.001$) was found in 20 paired PTC tissues (Additional file 8: Fig S4A). Thus, on the basis of above observation, CDH4 was confirmed as a target of miR-612 and therefore was regulated by FER1L4.

FER1L4/miR-612/CDH4 axis promotes PTC cell proliferation and invasion

It is clear that the expression of CDH4 was upregulated in PTC tissues and cell lines (Additional file 8: Fig S4B-C). To delineate further the functional significance of CDH4 in PTC cell proliferation and invasion, the expression of CDH4 was efficiently knocked down in K-1 and TPC-1 cells (Fig. 6F; Additional file 8: Fig S4D). Firstly, loss of CDH4 repressed cell proliferation as presented by EdU incorporation (Fig. 6G; Additional file 8: Fig S4E) and CCK8 assays (Fig. 6H). Furthermore, silencing CDH4 displayed a significant induction in apoptosis (Fig. 6I; Additional file 8: Fig S4F) accompanied by elevated Bax expression and reduced Bcl2 expression, as well as cell cycle arrest at S phase (Fig. 6J; Additional file 8: Fig S4G) with reduced proteins level of CDK2 and cyclinA2 (Fig. 6K and 7A). Importantly, subcutaneous tumor formation experiments revealed that knockdown of CDH4 significantly inhibited the formation of subcutaneous tumors of PTC cells (Fig. 7B; Additional file 8: Fig S4I). In addition, IHC assay also showed upregulated expression of CDH4 in PTC tissue samples (Fig. 7C). As expected, wound healing assays uncovered a reduction of cell migrative rate in CDH4 depleted cells (Fig. 7D). Consistently, transwell assays displayed a sharp decline in cell numbers getting through the chamber by knockdown of CDH4 (Fig. 7E). Together, these experiments support an oncogenic role for CDH4 in promoting PTC cell proliferation and invasion. Subsequently, we performed several cell functional experiments in CDH4 depleted cells with simultaneous knockdown of miR-612. First, co-transfected with miR-612 inhibitor in PTC cells resulted in a reversal of CDH4 siRNA-induced repression of cell growth (Fig. 7F). Then, we further examined the effect on cell metastatic ability. As indicated by transwell assays, CDH4 siRNA-mediated decrease in cell numbers were nullified by artificially lowered expression of miR-612 (Fig. 7G-I; Additional file 8: Fig S4J). In conclusion, these results suggested there may exist an axis between FER1L4, miR-612 and CDH4 which involves in the tumorigenesis and aggressiveness of papillary thyroid cancer.

Discussion

Thyroid cancer development involves multiple genetic and epigenetic alterations such as point mutation of the BRAF and RAS genes which seem to be linked to specific etiologic factors like exposure to ionizing radiation and chemical mutagenesis (23). In recent decades, technical advances in genome editing and high-throughput sequencing has promoted the deeply research of non-coding genomes (24). Notably, long noncoding RNA, the main components of non-coding genes, is considered to be essentially implicated in the process of tumor initiation or progression including thyroid cancer (25). Fer-1 like family member 4 is a lncRNA with 6.7 kb length, located in chromosome 20 q11.22. However, intriguingly, the literature documents context-dependent phenotype of FER1L4 in human cancers. It was previously reported that FER1L4 serves as tumor suppressor in colon (26) and gastric cancer (27), whereas promotes the proliferation and cell cycle of glioma cells (28). In a human pan-cancer analysis, it suggested FER1L4 may act as an oncogenic driver in human cancers (29). Thus, importantly, the current study unravels a new facet of FER1L4 which accelerates thyroid papillary cancer proliferation and metastasis. In agreement, upregulated expression of FER1L4 in PTC tissues was closely related to advanced clinicopathological features like lymph node metastasis, extrathyroidal extension, and

advanced TNM stage. Accordingly, FER1L4 plays an oncogenic role in PTC which could be new biomarkers and treatment target of PTC.

In our study, the confirmation that FER1L4 is located in cytoplasm give us reason to hypothesize that FER1L4 may influence the progression of thyroid papillary carcinoma through the mechanism model of ceRNA. Subsequently, miR-612 was validated to directly bind to FER1L4 in PTC cells via the dual luciferase reporter assay. MiR-612 has been proved to suppress tumor growth and metastasis in many tumors. For example, miR-612 negatively controlled the formation of invadopodia, matrix degradation and metastasis of hepatocellular carcinoma by HADHA-mediated lipid reprogramming (30). Nevertheless, the function of miR-612 in thyroid cancer has not been described before. Herein, in this study, miR-612 was also successfully identified as tumor suppressor which inhibits cell proliferation, migration and invasion of PTC. Meanwhile, functional experiments also suggested FER1L4-induced promotion of PTC cell is mediated by the negatively regulating to miR-612. Hence, our findings uncovered that FER1L4 exerts oncogenic behavior partly via sponging miR-612 in PTC cells.

Cadherin 4 was proved to be the target of miR-612 in this study. However, knockdown of FER1L4 or overexpression of miR-612 only influences the expression of CDH4 at the protein level, which indicates miR-612 may repress the translation of CDH4 and then attenuates its expression (31), yet the detailed mechanism of such regulation demand further exploration. Deregulation of CDH4 has been implicated in several human cancers. Dependent on the cell context, in most epithelial cancers like breast (32), colorectal and gastric cancer (33), CDH4 is epigenetically silenced by promoter hypermethylation and commonly suggested to act as a tumor suppressor. Nevertheless, some researches also support an oncogenic function of CDH4 in high-grade gliomas (17) and osteosarcoma (34). Although there are discrepancies to the function of CDH4 in human cancer, our study identifies and suggests CDH4 as an oncogenic driver in PTC that promotes PTC cell proliferation, migration, invasion and cell cycle progression. Consistent with its function in cell-cell adhesion, immunohistochemical analysis indicated that CDH4 shows crisp membrane localization in PTC tissues. In particular, Gene Set Enrichment Analysis (GSEA) of CDH4 using gene expression profile from TCGA database also invalidates that CDH4 involves in process of adherens junction and extracellular matrix-receptor interaction (Additional file 9: Fig S5A-B) (35). On the other hand, FER1L4 was also characterized that is positively related to gene set of cell adhesion molecules (Additional file 9: Fig S5C). However, person correlation analysis suggested FER1L4 expression positively correlates with the expression of P-cadherin ($R^2 = 0.2513$, $P < 0.001$) but not the others (E-cadherin, N-cadherin and CDH4) (Additional file 9: Fig S5E-H), which was consistent with the RT-PCR results (Fig. 6A). Intriguingly, the expression of CDH4 also positively correlated with P-cadherin using TCGA database ($R^2 = 0.1156$, $P < 0.001$; Additional file 9: Fig S5K), indicating that FER1L4 may regulate the expression of P-cadherin via governing CDH4 or vice versa (36). However, it needs further experimental confirmation. Meanwhile, to elucidate the mechanism of CDH4-induced PTC cell proliferation is an important topic either. It was reported that CDH4 is necessary to the activation of ERK and p27 (17) and also the activation of c-Jun (34). GSEA analysis also suggested that CDH4 positively correlates with the wnt/β-catenin pathway, which may explain the promotion to PTC cells of CDH4 either

(Additional file 9: Fig S5D). Collectively, different expression level and function of FER1L4 and CDH4 in human cancers may be caused by the heterogeneity of tumors (37), which suggesting the great potential of FER1L4 and CDH4 as diagnostic biomarkers. Additionally, the underlying mechanism of CDH4 in PTC carcinogenesis requires thoroughly exploration.

Conclusions

Taken together, we identified that FER1L4 promotes PTC development via working as a sponge for miR-612 to attenuate its repressive effect on CDH4. These results provide a better understanding of the role of lncRNA in thyroid cancer progression, as well as a potential therapeutic and diagnostic target.

Abbreviations

LncRNAs: Long noncoding RNAs,

PTC: Papillary thyroid cancer,

CDH4: Cadherin 4

TC: Thyroid cancer

DTC: Differentiated thyroid cancer

FER1L4: Fer-1 like family member 4

E-cadherin, CDH1: Epithelial-cadherin

N-cadherin, CDH2: Neural-cadherin

P-cadherin, CDH3: Placental-cadherin

EMT: Epithelial-Mesenchymal Transition

siRNA: Small interfering RNA

ceRNA: Competing endogenous RNAs

FISH: Fluorescence in situ hybridization

RIP: RNA immunoprecipitation

Declarations

Ethics approval and consent to participate

This study was reviewed and approved by the Ethics Committee of the First Affiliated Hospital of Nanjing Medical University. Written informed consent was obtained from each patient.

Consent for publication

All authors agree to submit the article for publication.

Availability of data and materials

The datasets used and/or analyzed during the current study are available from the corresponding author on reasonable request.

Conflict of interest

The authors declare that they have no conflict of interest.

Funding

This study was supported by grants from the Nanjing Medical University Science and Technology Development Fund-Specialized Disease Cohort (NMUC2018019A), and the General Project of Jiangsu Provincial Department of Health (H2018057).

Author contributions

L Wu and Y Ding designed this study. L Wu, Y Ding and M Shen were responsible for the interpretation of the results. J Cai, H Tong, Y Si, H Zhang, X Wang processed the data processing and performed the statistical analysis. L Wu wrote the manuscript. X Zhuang and M Shen revised and improved the manuscript. M Shen for the supervision. All authors approved the submission.

References

1. Bray F, Ferlay J, Soerjomataram I, Siegel RL, Torre LA, Jemal A. Global cancer statistics 2018: GLOBOCAN estimates of incidence and mortality worldwide for 36 cancers in 185 countries. CA Cancer J Clin. 2018;68(6):394-424.
2. Haugen BR, Alexander EK, Bible KC, Doherty GM, Mandel SJ, Nikiforov YE, et al. 2015 American Thyroid Association Management Guidelines for Adult Patients with Thyroid Nodules and Differentiated Thyroid Cancer: The American Thyroid Association Guidelines Task Force on Thyroid Nodules and Differentiated Thyroid Cancer. Thyroid. 2016;26(1):1-133.

3. Lim H, Devesa SS, Sosa JA, Check D, Kitahara CM. Trends in Thyroid Cancer Incidence and Mortality in the United States, 1974-2013. JAMA. 2017;317(13):1338-48.
4. Links TP, van Tol KM, Jager PL, Plukker JT, Piers DA, Boezen HM, et al. Life expectancy in differentiated thyroid cancer: a novel approach to survival analysis. Endocr Relat Cancer. 2005;12(2):273-80.
5. Kreissl MC, Janssen MJR, Nagarajah J. Current Treatment Strategies in Metastasized Differentiated Thyroid Cancer. J Nucl Med. 2019;60(1):9-15.
6. Geisler S, Coller J. RNA in unexpected places: long non-coding RNA functions in diverse cellular contexts. Nature reviews Molecular cell biology. 2013;14(11):699-712.
7. Bhan A, Soleimani M, Mandal SS. Long Noncoding RNA and Cancer: A New Paradigm. Cancer Res. 2017;77(15):3965-81.
8. Boon RA, Jae N, Holdt L, Dimmeler S. Long Noncoding RNAs: From Clinical Genetics to Therapeutic Targets? J Am Coll Cardiol. 2016;67(10):1214-26.
9. Kang CL, Qi B, Cai QQ, Fu LS, Yang Y, Tang C, et al. LncRNA AY promotes hepatocellular carcinoma metastasis by stimulating ITGAV transcription. Theranostics. 2019;9(15):4421-36.
10. Liang Y, Song X, Li Y, Chen B, Zhao W, Wang L, et al. LncRNA BCRT1 promotes breast cancer progression by targeting miR-1303/PTBP3 axis. Molecular cancer. 2020;19(1):85.
11. Chen LL. Linking Long Noncoding RNA Localization and Function. Trends Biochem Sci. 2016;41(9):761-72.
12. Yao RW, Wang Y, Chen LL. Cellular functions of long noncoding RNAs. Nat Cell Biol. 2019;21(5):542-51.
13. Qin Y, Sun W, Wang Z, Dong W, He L, Zhang T, et al. ATF2-Induced lncRNA GAS8-AS1 Promotes Autophagy of Thyroid Cancer Cells by Targeting the miR-187-3p/ATG5 and miR-1343-3p/ATG7 Axes. Molecular therapy Nucleic acids. 2020;22:584-600.
14. Colas-Algora N, Millan J. How many cadherins do human endothelial cells express? Cell Mol Life Sci. 2019;76(7):1299-317.
15. Kaszak I, Witkowska-Pilaszewicz O, Niewiadomska Z, Dworecka-Kaszak B, Ngosa Toka F, Jurka P. Role of Cadherins in Cancer-A Review. Int J Mol Sci. 2020;21(20).
16. Kourtidis A, Lu R, Pence LJ, Anastasiadis PZ. A central role for cadherin signaling in cancer. Exp Cell Res. 2017;358(1):78-85.
17. Appolloni I, Barilari M, Caviglia S, Gambini E, Reisoli E, Malatesta P. A cadherin switch underlies malignancy in high-grade gliomas. Oncogene. 2015;34(15):1991-2002.
18. Zhuang X, Tong H, Ding Y, Wu L, Cai J, Si Y, et al. Long noncoding RNA ABHD11-AS1 functions as a competing endogenous RNA to regulate papillary thyroid cancer progression by miR-199a-5p/SLC1A5 axis. Cell death & disease. 2019;10(8):620.
19. Huang HY, Chien CH, Jen KH, Huang HD. RegRNA: an integrated web server for identifying regulatory RNA motifs and elements. Nucleic acids research. 2006;34(Web Server issue):W429-34.

20. Jeggari A, Marks DS, Larsson E. miRcode: a map of putative microRNA target sites in the long non-coding transcriptome. Bioinformatics (Oxford, England). 2012;28(15):2062-3.
21. Li JH, Liu S, Zhou H, Qu LH, Yang JH. starBase v2.0: decoding miRNA-ceRNA, miRNA-ncRNA and protein-RNA interaction networks from large-scale CLIP-Seq data. Nucleic acids research. 2014;42(Database issue):D92-7.
22. Sticht C, De La Torre C, Parveen A, Gretz N. miRWalk: An online resource for prediction of microRNA binding sites. PLoS One. 2018;13(10):e0206239.
23. Nikiforov YE, Nikiforova MN. Molecular genetics and diagnosis of thyroid cancer. Nature Reviews Endocrinology. 2011;7(10):569-80.
24. Djebali S, Davis CA, Merkel A, Dobin A, Lassmann T, Mortazavi A, et al. Landscape of transcription in human cells. Nature. 2012;489(7414):101-8.
25. Sedaghati M, Kebebew E. Long noncoding RNAs in thyroid cancer. Current opinion in endocrinology, diabetes, and obesity. 2019;26(5):275-81.
26. Yue B, Sun B, Liu C, Zhao S, Zhang D, Yu F, et al. Long non-coding RNA Fer-1-like protein 4 suppresses oncogenesis and exhibits prognostic value by associating with miR-106a-5p in colon cancer. Cancer Sci. 2015;106(10):1323-32.
27. Xu J, Li N, Deng W, Luo S. Long noncoding RNA FER1L4 suppresses proliferation, invasion, migration and lymphatic metastasis of gastric cancer cells through inhibiting the Hippo-YAP signaling pathway. American journal of translational research. 2020;12(9):5481-95.
28. Xia L, Nie D, Wang G, Sun C, Chen G. FER1L4/miR-372/E2F1 works as a ceRNA system to regulate the proliferation and cell cycle of glioma cells. Journal of cellular and molecular medicine. 2019;23(5):3224-33.
29. You Z, Ge A, Pang D, Zhao Y, Xu S. Long noncoding RNA FER1L4 acts as an oncogenic driver in human pan-cancer. Journal of cellular physiology. 2020;235(2):1795-807.
30. Liu Y, Lu LL, Wen D, Liu DL, Dong LL, Gao DM, et al. MiR-612 regulates invadopodia of hepatocellular carcinoma by HADHA-mediated lipid reprogramming. J Hematol Oncol. 2020;13(1):12.
31. Lee YS, Dutta A. MicroRNAs in cancer. Annu Rev Pathol. 2009;4:199-227.
32. Agiostratidou G, Li M, Suyama K, Badano I, Keren R, Chung S, et al. Loss of retinal cadherin facilitates mammary tumor progression and metastasis. Cancer Res. 2009;69(12):5030-8.
33. Miotto E, Sabbioni S, Veronese A, Calin GA, Gullini S, Liboni A, et al. Frequent aberrant methylation of the CDH4 gene promoter in human colorectal and gastric cancer. Cancer Res. 2004;64(22):8156-9.
34. Tang Q, Lu J, Zou C, Shao Y, Chen Y, Narala S, et al. CDH4 is a novel determinant of osteosarcoma tumorigenesis and metastasis. Oncogene. 2018;37(27):3617-30.
35. Mège RM, Ishiyama N. Integration of Cadherin Adhesion and Cytoskeleton at Adherens Junctions. Cold Spring Harbor perspectives in biology. 2017;9(5).
36. Martinez-Garay I, Gil-Sanz C, Franco SJ, Espinosa A, Molnar Z, Mueller U. Cadherin 2/4 signaling via PTP1B and catenins is crucial for nucleokinesis during radial neuronal migration in the neocortex.

Development. 2016;143(12):2121-34.

37. Meacham CE, Morrison SJ. Tumour heterogeneity and cancer cell plasticity. Nature. 2013;501(7467):328-37.

Figures

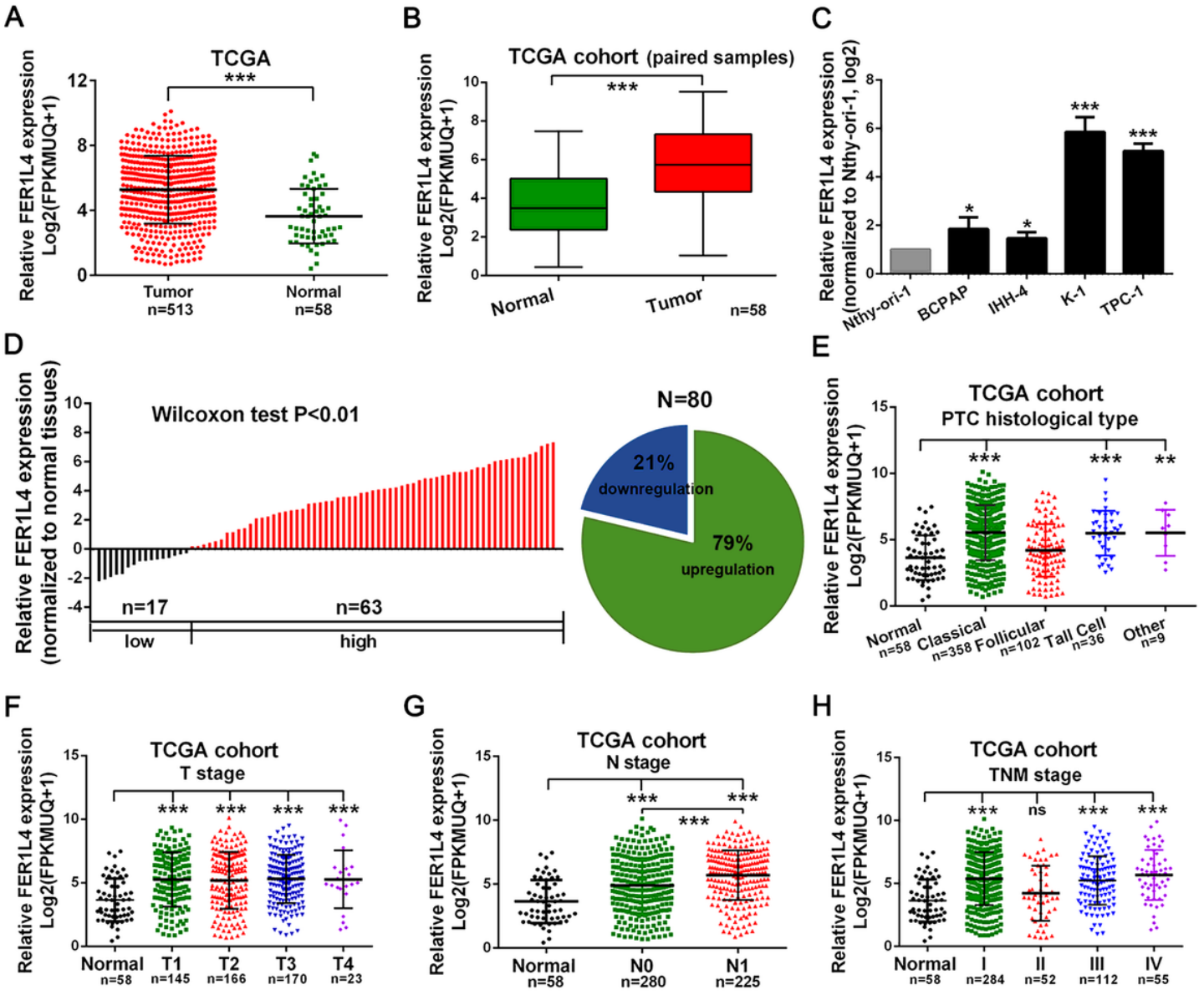

Figure 1

FER1L4 is upregulated in PTC and associated with advanced stage. A-B The expression of FER1L4 was upregulated in unpaired (A) or paired (B) PTC tissue samples based on TCGA database. C Enhanced expression level of FER1L4 was detected in PTC cell lines. D qRT-PCR analysis of 80 paired PTC tissue samples. E-H Expression patterns of FER1L4 based on histological type (E), T stage (F), N stage (G) and TNM stage (H) from TCGA database. Error bars, mean ± SD. *, P < 0.05; **, P < 0.01; ***, P<0.001.

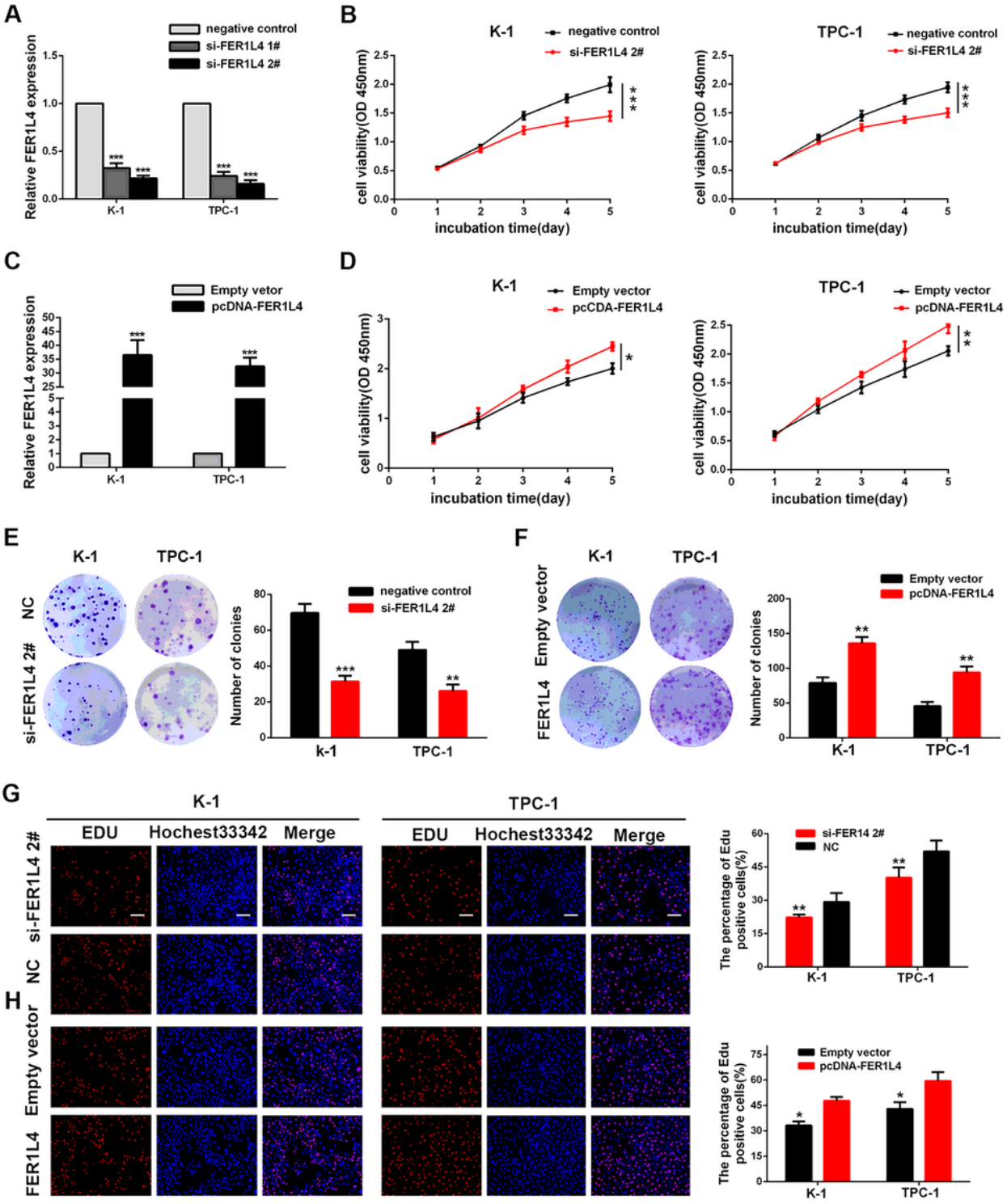

Figure 2

FER1L4 promotes PTC cell proliferation. A The expression of FER1L4 was efficiently knocked down. B Knockdown of FER1L4 inhibited K-1 and TPC-1 cell growth. C Artificially enhanced expression of FER1L4 in PTC cells. D The proliferation of PTC cells treated with FER1L4 vector was measured by cell counting kit 8 assays. E-F colony-formation numbers of PTC cells transfected with FER1L4 targeting siRNA (E) and FER1L4 expression vector (F). G-H cell proliferation measured by EdU incorporation assays in K-1 and

TPC-1 cells treated with FER1L4 targeting siRNA (G) and FER1L4 expression vector (H), 100×, Scale bars =100μm. Error bars, mean ± SD. *, P < 0.05; **, P < 0.01; ***, P<0.001.

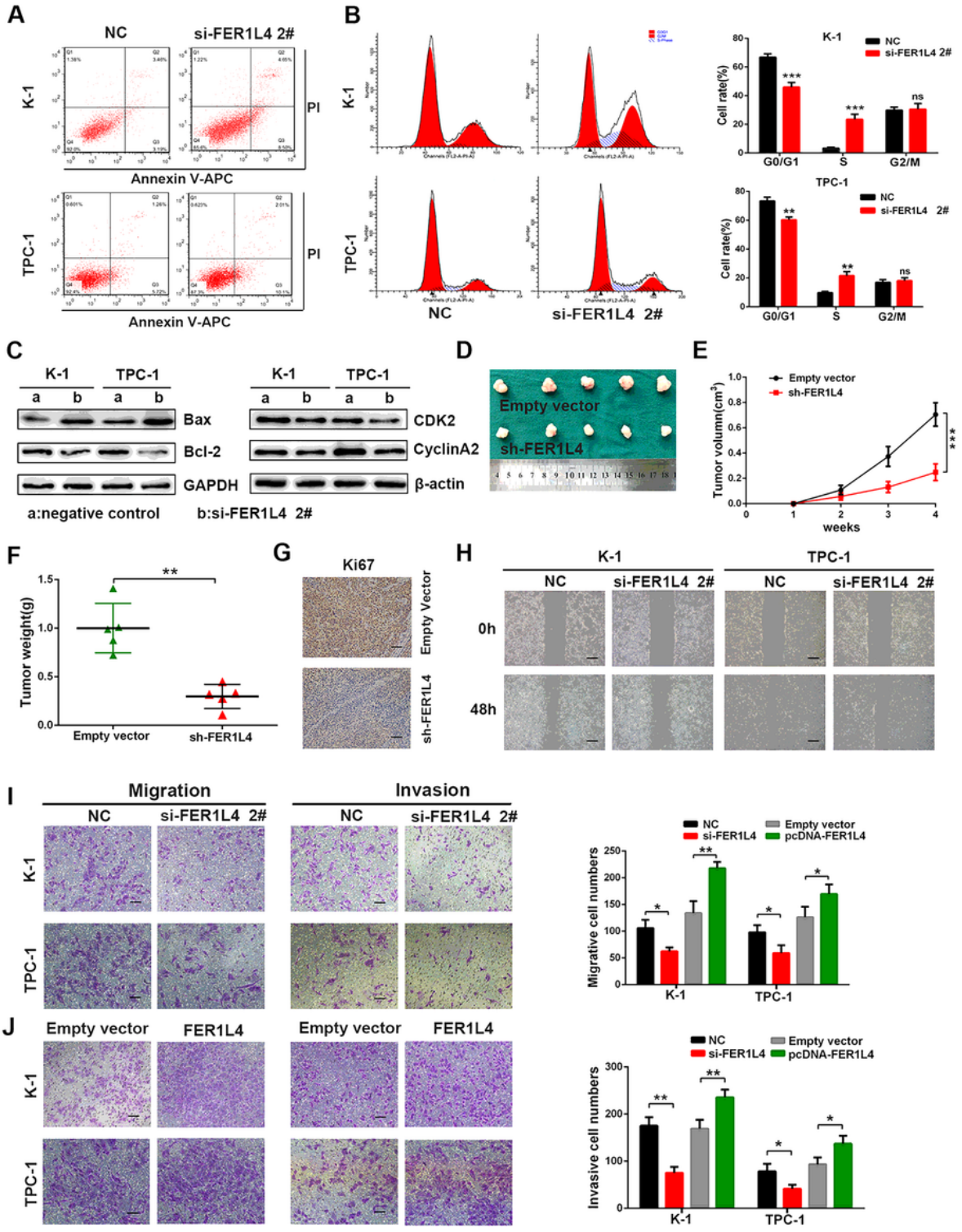

Figure 3

Effects of FER1L4 on cell apoptosis, cell cycle arrest, cell migration and invasion. A-B Flow cytometric analysis in apoptotic rate (A) and cell cycle arrest (B) of K-1 and TPC-1 cells transfected with FER1L4 targeting siRNA. C Expression level of apoptosis-related markers and S phase checkpoint protein in PTC

cells after depletion of FER1L4. D-F Tumor growth in mice subcutaneously implanted FER1L4-knockdown TPC-1 cells, and the tumor image (D), growth curve (E) and weight (F) are shown (n=5). G Representative image of immunohistochemistry analysis of Ki67 in implanted tumors, 100×, Scale bars=100μm. H Effects of silencing FER1L4 on cell migration by wound healing assay. I-J Transwell migration and invasion assays were conducted to investigate the influence of silencing FER1L4 (I) or overexpression of FER1L4 (J), 100×, Scale bars=100μm. Error bars, mean ± SD. *, P < 0.05; **, P < 0.01; ***, P<0.001.

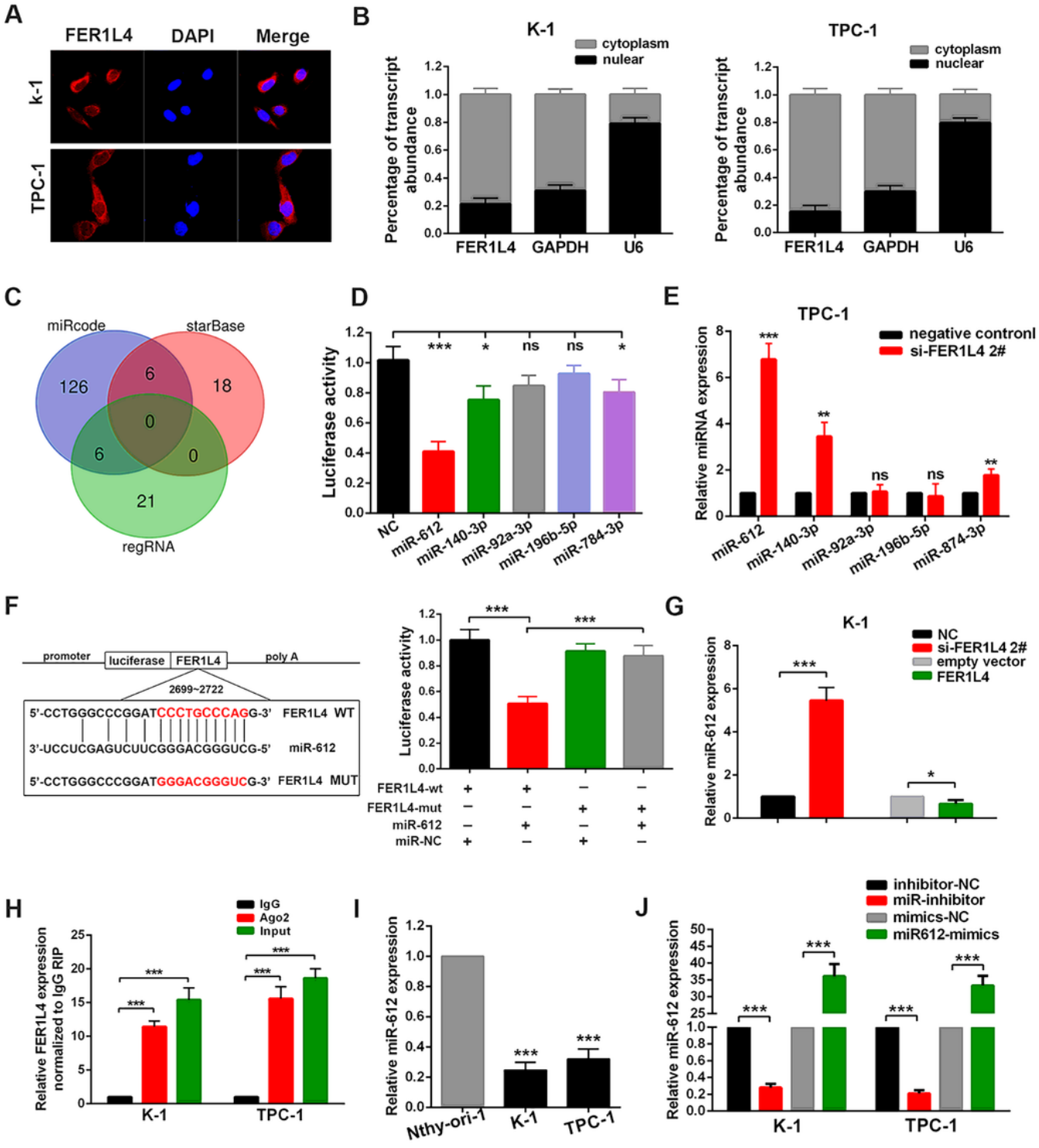

Figure 4

miR-612 is sponged by FER1L4 in PTC. A The location of FER1L4 in PTC cells as suggested by in situ hybridization assay. Nuclei was stained by DAPI as blue, and FER1L4 was labeled by Cy3 as red. Scale bars represent 50μm. B qRT-PCR analysis of FER1L4 in different subcellular fractions. U6 and GAPDH were used as nuclear and cytoplasmic markers, respectively. C Potential miRNAs with binding sites to FER1L4 were predicted by online tools. D Luciferase activity was detected in PTC cells cotransfected with miRNA mimics and luciferase reporter plasmid. E The expression level of potential miRNA after knockdown of FER1L4 in TPC-1 cells. F Schematic diagram representing the predicted binding sites and mutant sequence for miR-612 in FER1L4 (left panel). Indicated luciferase vector and miR-612 mimics were transduced into PTC cells and luciferase activity was detected (right panel). G Expression level of miR-612 as indicated. H Anti-Ago2 RIP assays were performed in PTC cells, followed by RT-PCR to detect the expression of FER1L4 in the immunoprecipitates. I Expression level of miR-612 in K-1 and TPC-1 cells compared with Nthy-ori-1. J Expression level of miR-612 in cells treated with miR-612 inhibitor and mimics. Error bars, mean ± SD. *, $P < 0.05$; **, $P < 0.01$; ***, $P<0.001$.

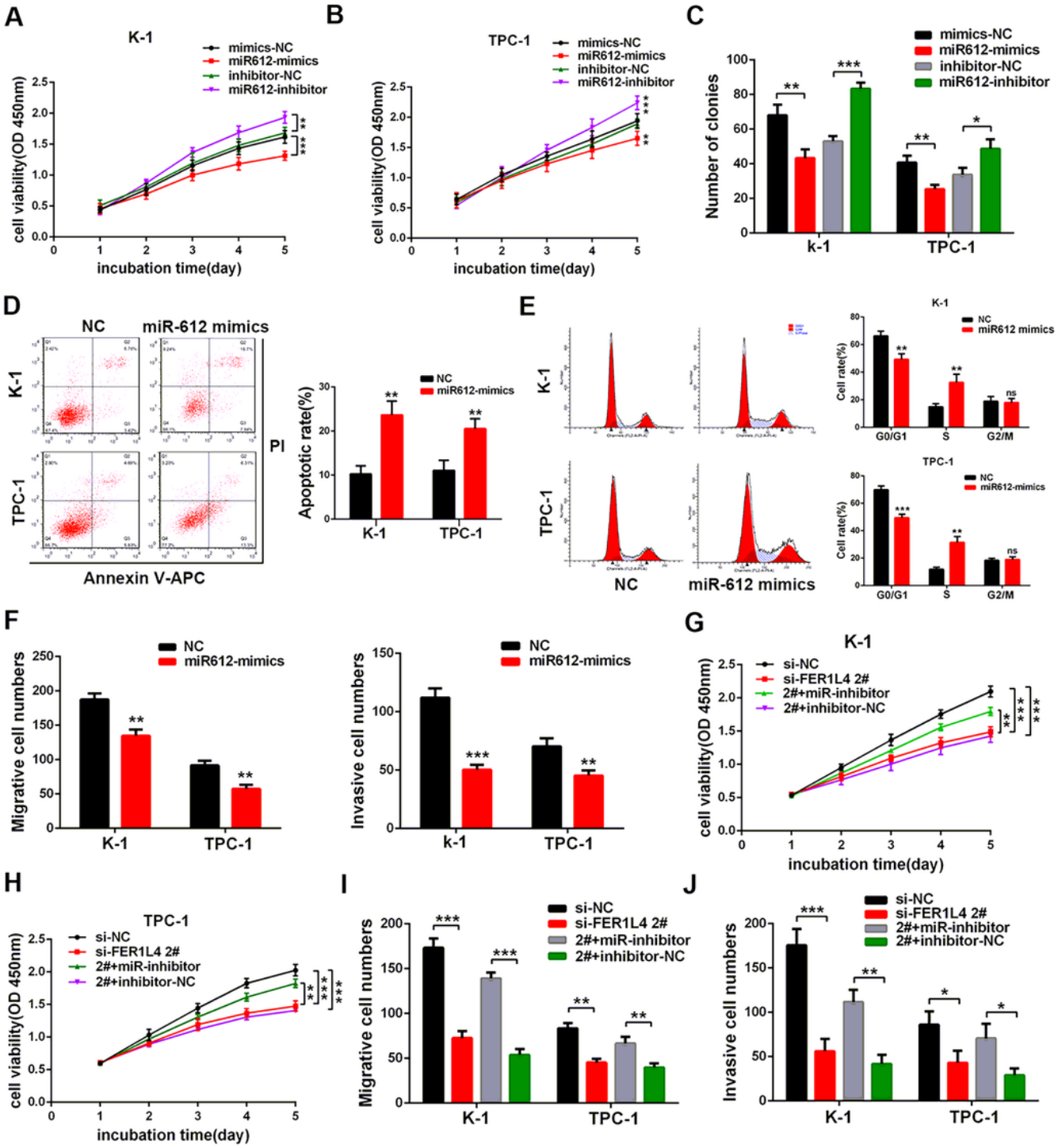

Figure 5

FER1L4 requires miR-612 to promote PTC cell growth and metastasis. A-B Detection of cell proliferation in K-1 (A) and TPC-1 cells (B) treated with miR-612 inhibitor and mimics as indicated. C Colony formation assay was performed to evaluate the effect of miR-612 on cell growth. D-E Overexpression of miR-612 induced cell apoptosis (D) and cell cycle arrest at S phase (E). F Ectopic expression of miR-612 promoted PTC cell migration and invasion in transwell assays. G-H miR-612 rescue the effects of FER1L4 on K-1

(G) and TPC-1 (H) cell proliferation as indicated by CCK8 assays. I-J Transwell assay was used to determine the migration (I) and invasion (J) of PTC cells cotransfected with FER1L4 and miR-612. Error bars, mean ± SD. *, P < 0.05; **, P < 0.01; ***, P<0.001.

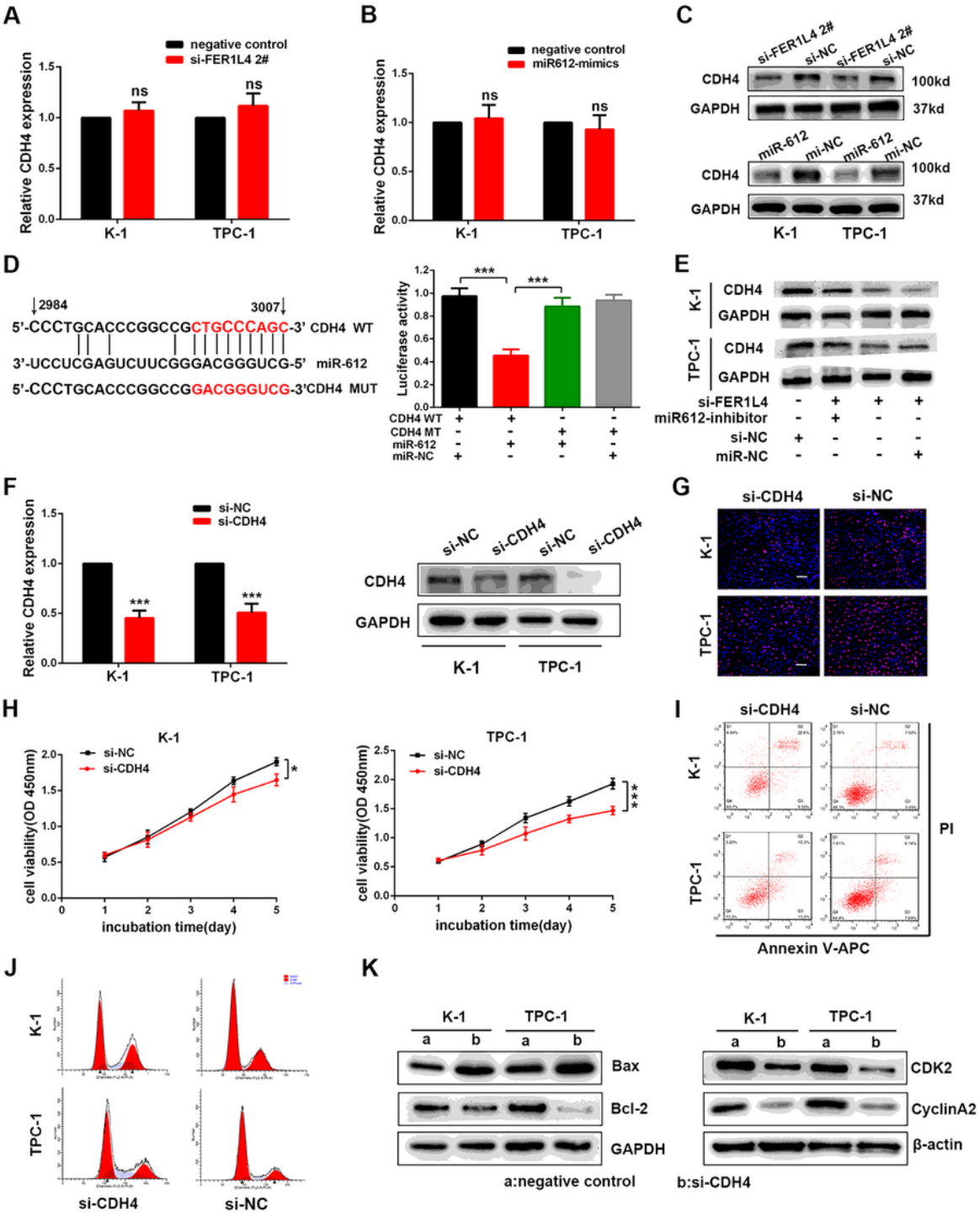

Figure 6

FER1L4 upregulates CDH4 expression via inhibition of miR-612. A-B Expression level of CDH4 after knockdown of FER1L4 (A) and overexpression of miR-612 (B). C Western blot analysis of CDH4 protein

level in PTC cells treated with FER1L4-targeting siRNA or miR-612 mimics. D The binding sites of miR-612 to FER1L4 3'UTR were mutated (left panel), and then the luciferase activity in TPC-1 cells with or without miR-612 overexpression and transfected with the WT or MUT luciferase plasmids were detected (right panel). E Western blot analysis of CDH4 protein level in PTC cells cotransfected with FER1L4 siRNA and miR-612 inhibitor. F The RNA and protein level of CDH4 were both silenced by CDH4-targeting siRNA. G-H The proliferation of K-1 and TPC-1 cells transfected with siRNA against CDH4 were measured using EdU incorporation assays (G), CCK8 assays (H), 100×, Scale bars =100μm. I-J Flow cytometric analysis of cell apoptosis (I) and cell cycle (J) to cells treated with CDH4-targeting siRNA. K Relative expression of Bax, Bcl-2, CDK2 and CyclinA2 in CDH4 depleted PTC cells compared with control. Error bars, mean ± SD. *, $P < 0.05$; **, $P < 0.01$; ***, $P<0.001$.

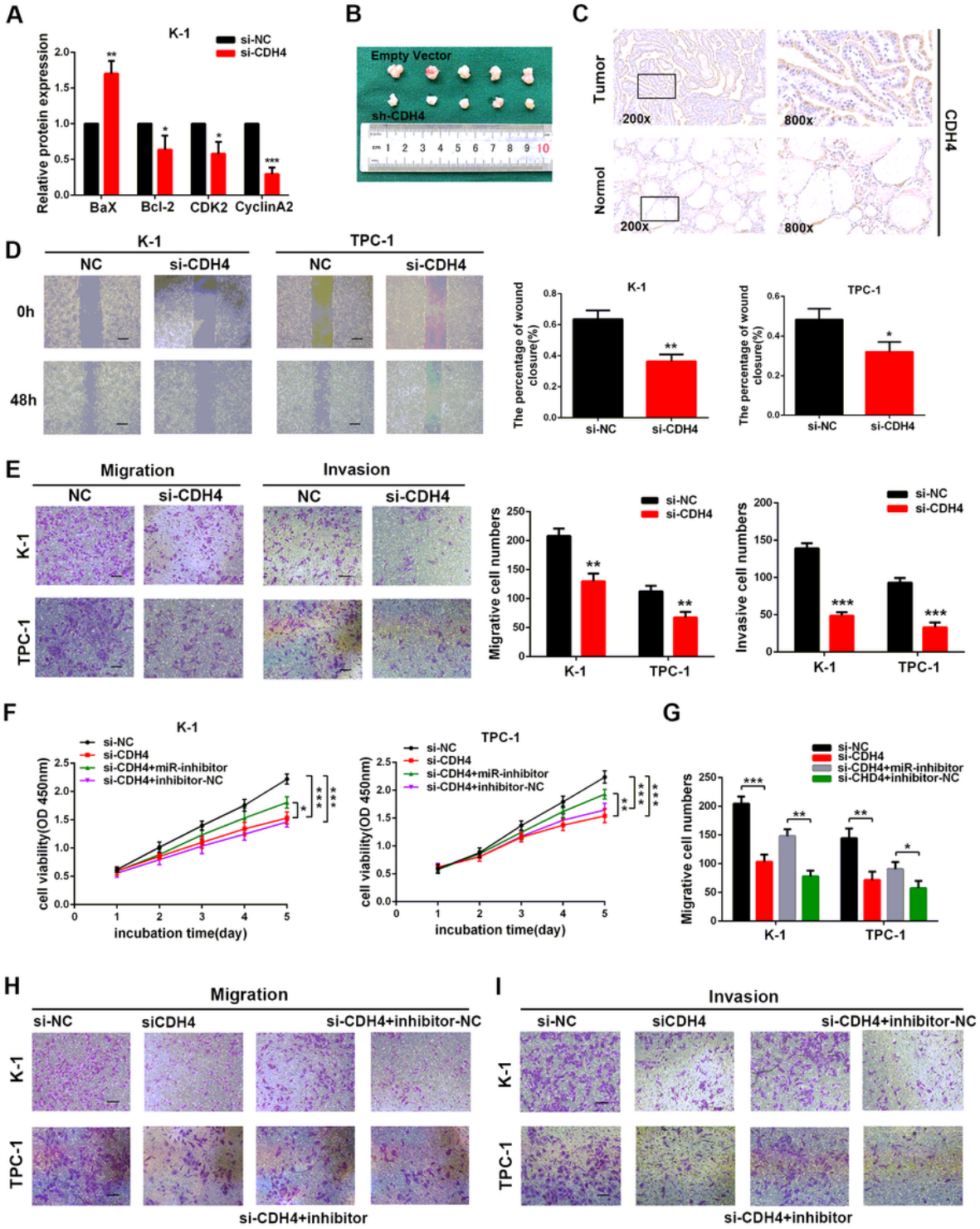

Figure 7

CDH4 promotes PTC cell proliferation and metastasis. A Quantitative analysis of the expression of Bax, Bcl-2, CDK2 and CyclinA2 after knockdown of CDH4. B Implanted tumors in mice were harvested and photographed. C Immunohistochemistry analysis of CDH4 expression in PTC tissues and adjacent normal tissues. D-E Knockdown of CDH4 inhibited PTC cell migration and invasion as suggested by wound healing assays (D) and transwell assays (E). 100×, Scale bars=100μm. F Rescue effects of miR-

612 inhibitor on CDH4 siRNA-mediated inhibition of cell proliferation in K-1 and TPC-1 cells determined by CCK8 assays. G-I Rescue effects of miR-612 inhibitor on CDH4 siRNA-mediated inhibition of cell migration (G, H) and invasion (I) in PTC cells detected by transwell assays. Error bars, mean ± SD. *, P < 0.05; **, P < 0.01; ***, P<0.001.

Supplementary Files

This is a list of supplementary files associated with this preprint. Click to download.

- Additionalfile1TableS1.docx
- Additionalfile2TableS2.docx
- Additionalfile3TableS3.docx
- Additionalfile4TableS4.docx
- Additionalfile5FigS1.docx
- Additionalfile6FigS2.docx
- Additionalfile7FigS3.docx
- Additionalfile8FigS4.docx
- Additionalfile9FigS5.docx